

performed in the presence of picrotoxin (100 μ M) unless indicated otherwise. Monosynaptic EPSPs exhibiting constant 10–90% rise times and latencies were elicited by stimulation of afferent fibres with a bipolar twisted platinum/10% iridium wire (25 μ m diameter). LTP was quantified for statistical comparisons by normalizing and averaging EPSP slopes during the last 10 min of experiments relative to 5–10 min of baseline. Depicted traces show averaged EPSPs or EPSCs for 2 min of baseline and 2 min of LTP (20–25 min after pairing). All values are expressed as means \pm s.e.m. Statistical comparisons were done with paired or unpaired Student's *t*-test as appropriate (two-tailed *P* < 0.05 was considered significant). For details on experimental conditions and analysis see Supplementary Information.

Received 18 August; accepted 24 October 2003; doi:10.1038/nature02194.

1. Gustafsson, B. & Wigström, H. Basic features of long-term potentiation in the hippocampus. *Semin. Neurosci.* **2**, 321–333 (1990).
2. Bliss, T. V. P. & Collingridge, G. L. A synaptic model of memory: long-term potentiation in the hippocampus. *Nature* **361**, 31–39 (1993).
3. Bailey, C. H., Giustetto, M., Huang, Y. Y., Hawkins, R. D. & Kandel, E. R. Is heterosynaptic modulation essential for stabilizing Hebbian plasticity and memory? *Nature Rev. Neurosci.* **1**, 11–20 (2000).
4. Artola, A. & Singer, W. Long-term depression of excitatory synaptic transmission and its relationship to long-term potentiation. *Trends Neurosci.* **16**, 480–487 (1993).
5. Scanziani, M., Malenka, R. C. & Nicoll, R. A. Role of intercellular interactions in heterosynaptic long-term depression. *Nature* **380**, 446–450 (1996).
6. Tsukamoto, M. *et al.* Mossy fibre synaptic NMDA receptors trigger non-Hebbian long-term potentiation at entorhino-CA3 synapses in the rat. *J. Physiol. (Lond.)* **546**, 665–675 (2003).
7. Royer, S. & Paré, D. Conservation of total synaptic weight through balanced synaptic depression and potentiation. *Nature* **422**, 518–522 (2003).
8. Nishiyama, M., Hong, K., Mikoshiba, K., Poo, M. M. & Kato, K. Calcium stores regulate the polarity and input-specificity of synaptic modification. *Nature* **408**, 584–588 (2000).
9. LeDoux, J. E. Emotion circuits in the brain. *Annu. Rev. Neurosci.* **23**, 155–184 (2000).
10. Weisskopf, M. G., Bauer, E. P. & LeDoux, J. E. L-type voltage gated calcium channels mediate NMDA-independent associative long-term potentiation at thalamic input synapses to the amygdala. *J. Neurosci.* **19**, 10512–10519 (1999).
11. Bauer, E. P., Schafe, G. E. & LeDoux, J. E. NMDA receptors and L-type voltage gated calcium channels contribute to long-term potentiation and different components of fear memory formation in the lateral amygdala. *J. Neurosci.* **22**, 5239–5249 (2002).
12. Huang, Y. Y. & Kandel, E. R. Postsynaptic induction and PKA-dependent expression of LTP in the lateral amygdala. *Neuron* **21**, 169–178 (1998).
13. Quirk, G. J., Armony, J. L. & LeDoux, J. E. Fear conditioning enhances different temporal components of tone-evoked spike trains in auditory cortex and lateral amygdala. *Neuron* **19**, 613–624 (1997).
14. Rosenkranz, J. A. & Grace, A. A. Dopamine-mediated modulation of odour-evoked amygdala potentials during pavlovian conditioning. *Nature* **417**, 282–287 (2002).
15. Berretta, N. & Jones, R. S. Tonic facilitation of glutamate release by presynaptic N-methyl-D-aspartate autoreceptors in the entorhinal cortex. *Neuroscience* **75**, 339–344 (1996).
16. Lang, E. J. & Paré, D. Similar inhibitory processes dominate the responses of cat lateral amygdaloid projection neurons to their various afferents. *J. Neurophysiol.* **77**, 341–352 (1997).
17. Szinyei, C., Heinbockel, T., Montagne, J. & Pape, H. C. Putative cortical and thalamic inputs elicit convergent excitation in a population of GABAergic interneurons of the lateral amygdala. *J. Neurosci.* **20**, 8909–8915 (2000).
18. Abraham, W. C. & Wickens, J. R. Heterosynaptic long-term depression is facilitated by blockade of inhibition in area CA1 of the hippocampus. *Brain Res.* **546**, 336–340 (1991).
19. Lang, E. J. & Paré, D. Synaptic responsiveness of interneurons of the cat lateral amygdaloid nucleus. *Neuroscience* **83**, 877–889 (1998).
20. Bissière, S., Humeau, Y. & Lüthi, A. Dopamine gates LTP induction in lateral amygdala by suppressing feedforward inhibition. *Nature Neurosci.* **6**, 587–592 (2003).
21. McDonald, A. J. & Mascagni, F. Immunohistochemical localization of the β 2 and β 3 subunits of the GABA_A receptor in the basolateral amygdala of the rat and monkey. *Neuroscience* **75**, 407–419 (1996).
22. Farb, C. R., Aoki, C. & LeDoux, J. E. Differential localization of NMDA and AMPA receptor subunits in the lateral and basal nuclei of the amygdala: a light and electron microscopic study. *J. Comp. Neurol.* **362**, 86–108 (1995).
23. Gracy, K. N. & Pickel, V. M. Ultrastructural localization of NMDAR1 glutamate receptor immunoreactivity in the extended amygdala. *J. Comp. Neurol.* **362**, 71–85 (1995).
24. Farb, C. R. & LeDoux, J. E. Afferents from the rat temporal cortex synapse on lateral amygdala neurons that express AMPA and NMDA receptors. *Synapse* **33**, 218–229 (1999).
25. Hess, G., Kuhnt, U. & Voronin, L. L. Quantal analysis of paired-pulse facilitation in guinea pig hippocampal slices. *Neurosci. Lett.* **77**, 187–192 (1987).
26. Tsvetkov, E., Carlezon, W. A., Benes, F. M., Kandel, E. R. & Bolshakov, V. Y. Fear conditioning occludes LTP-induced presynaptic enhancement of synaptic transmission in the cortical pathway to the lateral amygdala. *Neuron* **34**, 289–300 (2002).
27. Humeau, Y., Popoff, M. R., Kojima, H., Doussau, F. & Poulain, B. Rac GTPase plays an essential role in exocytosis by controlling the fusion competence of release sites. *J. Neurosci.* **22**, 7968–7981 (2002).
28. Doyère, V., Schafe, G. E., Sigurdsson, T. & LeDoux, J. E. Long-term potentiation in freely moving rats reveals asymmetries in thalamic and cortical inputs to the lateral amygdala. *Eur. J. Neurosci.* **17**, 2703–2715 (2003).
29. Markram, H., Lübke, J., Frotscher, M. & Sakman, B. Regulation of synaptic efficacy by coincidence of postsynaptic APs and EPSPs. *Science* **75**, 213–215 (1997).
30. Blair, H. T., Schafe, G. E., Bauer, E. P., Rodrigues, S. M. & LeDoux, J. E. Synaptic plasticity in the lateral amygdala: a cellular hypothesis of fear conditioning. *Learn. Mem.* **8**, 229–242 (2001).

Supplementary Information accompanies the paper on www.nature.com/nature.

Acknowledgements We thank B. Gähwiler, C. Heuss, A. Matus, B. Poulain and E. Seifritz for discussions and comments on the manuscript. This work was supported by the Borderline Personality Disorder Research Foundation, the Swiss National Science Foundation and the Novartis Research Foundation.

Competing interests statement The authors declare that they have no competing financial interests.

Correspondence and requests for materials should be addressed to A.L. (andreas.luthi@fmi.ch).

.....

A microRNA controlling left/right neuronal asymmetry in *Caenorhabditis elegans*

Robert J. Johnston Jr & Oliver Hobert

Department of Biochemistry and Molecular Biophysics, Center for Neurobiology and Behavior, Columbia University, College of Physicians and Surgeons, 701 W.168th Street, New York, New York 10032, USA

.....

How left/right functional asymmetry is layered on top of an anatomically symmetrical nervous system is poorly understood. In the nematode *Caenorhabditis elegans*, two morphologically bilateral taste receptor neurons, ASE left (ASEL) and ASE right (ASER), display a left/right asymmetrical expression pattern of putative chemoreceptor genes that correlates with a diversification of chemosensory specificities^{1,2}. Here we show that a previously undefined microRNA termed *lisy-6* controls this neuronal left/right asymmetry of chemosensory receptor expression. *lisy-6* mutants that we retrieved from a genetic screen for defects in neuronal left/right asymmetry display a loss of the ASEL-specific chemoreceptor expression profile with a concomitant gain of the ASER-specific profile. A *lisy-6* reporter gene construct is expressed in less than ten neurons including ASEL, but not ASER. *lisy-6* exerts its effects on ASEL through repression of *cog-1*, an Nkx-type homeobox gene, which contains a *lisy-6* complementary site in its 3' untranslated region and that has been shown to control ASE-specific chemoreceptor expression profiles³. *lisy-6* is the first microRNA to our knowledge with a role in neuronal patterning, providing new insights into left/right axis formation.

Bilateral symmetry is a common feature of nervous system anatomy across phylogeny. Morphological symmetry is contrasted by the lateralization of many different nervous system functions, as well as by left/right asymmetrical patterns of gene expression^{4–6}. However, in only a very few cases have these asymmetrical gene expression patterns been specifically correlated with functional lateralization. One such example is provided by a bilaterally symmetrical class of taste receptor neurons, the ASE class^{7,8}, which displays left/right asymmetrical expression patterns of a family of putative chemoreceptors with guanylyl cyclase activity (Fig. 1a). In adult animals, the guanylyl cyclase receptor genes *gcy-6* and *gcy-7* are only expressed in ASEL, whereas *gcy-5* is only expressed in ASER¹. The asymmetry of *gcy* gene expression patterns correlates with a functional asymmetry of the ASEL and ASER neurons exemplified by their sensation of a different spectrum of chemosensory cues². The differential segregation of the chemosensory capacities in the left and right ASE neurons is required for intact behaviour in complex sensory environments. In mutant animals that exhibit a partial lateralization of chemoreceptor expression, chemosensation *per se* is unaffected, yet the ability to discriminate between individual chemosensory inputs is lost^{2,9}.

To elucidate how left/right asymmetrical expression of the *gcy*

chemoreceptors is established, we conducted a genetic screen for mutants in which the normally ASEL-specific expression of a *gcy-7^{prom}::gfp* reporter gene is disrupted³. One mutant retrieved from this screen, termed *lisy-6* (for laterally symmetrical), displays a 'two ASER' mutant phenotype, in which ASEL fails to show its normal expression of *gcy-7*, but instead expresses the normally ASER-specific *gcy-5* gene (Fig. 1b, c). Other aspects of ASE cell fate specification are unaffected (see below). Left/right asymmetrical olfactory receptor expression in the AWC neurons^{6,10} and directional left/right asymmetrical Q neuroblast migration⁶ is also unaffected in *lisy-6* mutants (data not shown).

Through standard three-factor mapping with a polymorphic *C. elegans* isolate¹¹, we mapped *lisy-6* to a 55-kilobase region between two single-nucleotide polymorphisms on chromosome V (Fig. 2a). After further narrowing the *lisy-6* locus through transformation rescue with DNA fragments from this region, we sequenced the locus in *lisy-6* mutants and uncovered a 1,071-base-pair (bp) deletion. Subfragments of the deleted region rescued the mutant phenotype, yet lacked any predicted protein product (Fig. 2a). Comparing the sequence of the rescuing fragments of *C. elegans* to the syntenic region of *Caenorhabditis briggsae*, a related nematode species, we identified a conserved inverted repeat that has the capacity to form a hairpin structure (Fig. 2b). Hairpin structures of this kind have previously been reported to be processed to 22/23-nucleotide-long microRNAs (miRNAs) that repress messenger RNA translation of specific target genes through binding to their 3' untranslated region (UTR)¹²⁻¹⁶. Within the *C. elegans* and *C. briggsae* hairpin structures lies a highly conserved 23-nucleotide sequence that probably forms a biologically active miRNA species. Outside of this 23-nucleotide region, the hairpin structures show limited primary sequence conservation but strong conservation of their secondary structures (Fig. 2b). Sequence similarity searches between the *lisy-6* hairpin or miRNA and the entries in the central miRNA registry (<http://www.sanger.ac.uk/Software/Rfam/mirna/search.shtml>) produced no hits, suggesting that *lisy-6* is a novel miRNA, not previously retrieved from either cloning or computer prediction approaches¹⁴⁻¹⁷.

A 521-bp fragment containing putative 5' transcriptional regulatory elements of the *lisy-6* locus and the *lisy-6* hairpin structure can

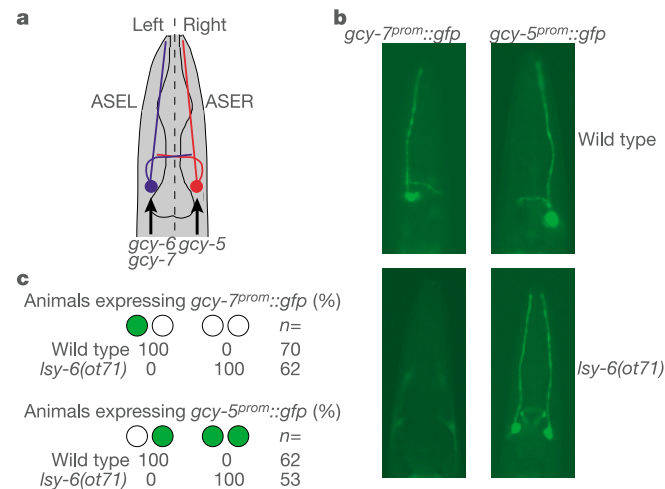


Figure 1 *lisy-6* regulates asymmetrical chemoreceptor gene expression. **a**, Gene expression asymmetry in the ASE class of chemosensory neurons. **b**, In *lisy-6(ot71)* mutants, *gcy-7^{prom}::gfp* expression is lost and *gcy-5^{prom}::gfp* expression is derepressed in ASEL. **c**, Quantification of *lisy-6(ot71)* effects on asymmetrical *gcy* expression. Circles represent ASEL and ASER, respectively, expressing either one of the indicated chromosomally integrated *gfp* reporter gene arrays. Animals were scored as adults.

rescue the asymmetry defect, both in terms of regaining *gcy-7* expression in ASEL and losing ectopic *gcy-5* expression in ASEL (Fig. 2a, fragment number 7). When the hairpin sequence is removed from a 781-bp rescuing fragment, rescue is lost (fragment number 9). Conversely, the hairpin sequence alone, without any flanking sequence, is not sufficient to rescue the asymmetry defect (fragment number 10), presumably owing to a lack of transcriptional regulatory elements. A substitution of four nucleotides in the stem of the hairpin abolishes *lisy-6* activity (*mut1*, fragment number 11). Furthermore, a single point mutation (*mut2*) in the hairpin removes the rescuing ability of the 781-bp fragment (number 12). Introduction of a compensatory mutation (*comp mut*) that restores hairpin secondary structure restores the rescuing activity (fragment number 13). Similarly, expression of the complete hairpin in one of the two possible orientations under control of a heterologous promoter is also able to restore ASEL fate (Fig. 3c). These experiments indicate that the hairpin is essential for *lisy-6* activity and that, by inference, *lisy-6* probably encodes a small regulatory RNA.

In order to identify the cellular focus of *lisy-6* action, we made use of the previous observation that miRNA expression can be monitored through RNA polymerase II-dependent transcriptional reporter constructs¹⁸. To this end, two kilobases of the 5' upstream

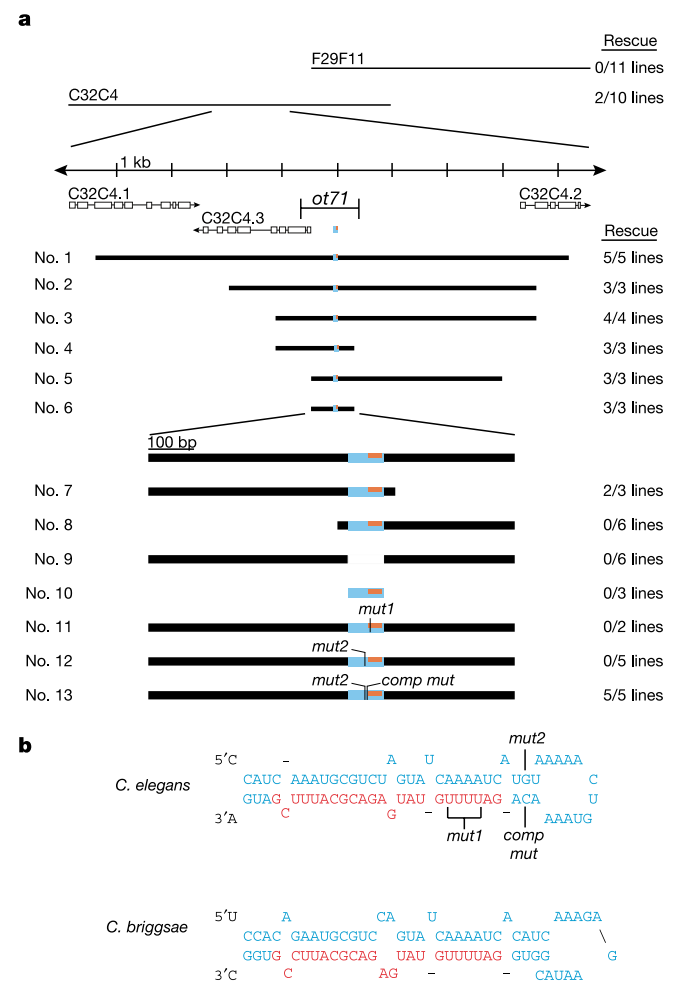


Figure 2 *lisy-6* encodes a novel miRNA. **a**, Transformation rescue of the *lisy-6* mutant phenotype monitored by *gcy-5^{prom}::gfp* expression. (See Supplementary Information for rescue assay.) The predicted miRNA hairpin is shown in blue, the 23-nucleotide miRNA in red. *mut1* is a UUUU to GGGG change, *mut2* is a G to C change, and *comp mut* is the compensatory C to G change in the opposite strand of the hairpin. **b**, Structure of the conserved *lisy-6* hairpin in *C. elegans* and *C. briggsae*. The *lisy-6* miRNA is highlighted in red.

region of the *lisy-6* hairpin (*lisy-6^{hairpin}*), which contain the regulatory elements required for rescue of the *lisy-6* mutant phenotype, were fused to *gfp*. Although reporter gene fusions can only be an approximation of endogenous gene expression patterns, we were intrigued to observe that adult transgenic animals expressing this reporter show only limited expression in one pair of tail neurons and in about seven head neurons (Fig. 3a). Of the head neurons, expression was consistently observed in ASEL but not in ASER in adult animals (Fig. 3b). To confirm the cell specificity of *lisy-6* action and the sufficiency to promote ASEL cell fate, we expressed *lisy-6* under the control of the *ceh-36* promoter (*ceh-36^{prom}*), which is expressed bilaterally in post-mitotic ASEL and ASER^{3,19}. Bilateral expression of *lisy-6* in ASEL and ASER in a *lisy-6* null mutant background is sufficient to not only restore *gcy-7* expression and repress ectopic *gcy-5* gene expression in ASEL, but also to repress normal *gcy-5* expression and induce *gcy-7* expression in ASER, thus illustrating the instructive nature of *lisy-6* function in determining asymmetrical chemoreceptor expression profiles (Fig. 3c, d). Reversing the orientation of the hairpin abolishes ASEL fate-inducing activity (Fig. 3c).

We have previously identified an antagonistic relationship between transcriptional repressor and activator proteins as part of a regulatory cascade that determines left/right asymmetry in ASE cells (Fig. 4g)^{3,9}. *cog-1*, an *Nkx6*-type homeobox transcription factor,

acts with the *groucho*-like transcriptional co-repressor *unc-37* to repress ASEL cell fate in ASER. This is achieved, at least in part, through the repression of the *lim-6* homeobox gene, which represses ASER fate (Fig. 4g)³. *ceh-36*, an OTX-type homeodomain transcription factor, and *lin-49*, a transcriptional co-activator, act to promote the left cell fate in ASEL (Fig. 4g)³. To order *lisy-6* into this regulatory hierarchy, we first analysed the expression of the three known cell-specific transcription factors *ceh-36*, *lim-6*, and *cog-1* in a *lisy-6(ot71)* null mutant background. Expression of the bilaterally expressed *ceh-36* gene was unaffected, confirming that the overall features of ASE cell fate are unaffected (Fig. 4b, e). Consistent with the conversion of ASEL to ASER cell fate, expression of the normally left-expressed *lim-6* gene is lost (Fig. 4a). Conversely, *cog-1*, a negative regulator of *lim-6*, which is normally expressed more strongly in ASER than in ASEL³, is derepressed in ASEL (Fig. 4b).

As *cog-1* is a negative regulator of *lim-6* in ASER³ and as its expression is derepressed in ASEL in *lisy-6* mutants, loss of *lim-6* expression in *lisy-6* mutants might be due to ectopic *cog-1* expression in ASEL. To test this notion experimentally, we removed *cog-1* activity in a *lisy-6* null mutant background and observed derepression of *lim-6* expression (Fig. 4c). We conclude that *lisy-6* acts through *cog-1* to affect *lim-6* expression (Fig. 4g).

We next asked whether *cog-1* is a direct target of *lisy-6*. Examining the 3' UTR of *cog-1*, we noted a single site with significant complementarity to *lisy-6* (Fig. 4d; a second site with significantly lower similarity is also present; data not shown). In spite of an overall lack of sequence similarity of the whole 3' UTR, this putative *lisy-6* target site shows marked conservation to a site in the 3' UTR of the *cog-1* orthologue in the related nematode *C. briggsae* (Fig. 4d), implying functional relevance of this site. Moreover, the site has strongest complementarity to the 5' region of the miRNA, recently described as a common feature of miRNA interactions with their cognate targets²⁰.

To test whether the *cog-1* 3' UTR is indeed targeted by *lisy-6*, we generated *gfp* reporters with heterologous 3' UTRs. As shown previously, a *ceh-36^{prom}::gfp::unc-54^{3'UTR}* reporter construct is expressed bilaterally in ASEL and ASER³. We substituted the *unc-54* 3' UTR with the *cog-1* 3' UTR and examined whether endogenous *lisy-6* was sufficient to repress GFP expression in ASEL by means of the *cog-1* 3' UTR. In nematodes carrying the *ceh-36^{prom}::gfp::cog-1^{3'UTR}* transgene, reporter expression in ASEL is downregulated compared with ASER in the same animal and when compared with ASEL in control animals (Fig. 4e). Downregulation of the reporter in ASEL is dependent on the presence of *lisy-6*, as reporter gene expression in ASEL of *lisy-6* mutants is derepressed to levels that are indistinguishable from the levels in ASER (Fig. 4e). Moreover, downregulation of the reporter is dependent on the presence of the *lisy-6* complementary site, as deletion of this site from the reporter results in defective downregulation in ASEL (Fig. 4e). These results demonstrate that *lisy-6* acts through the *lisy-6* complementary site in the *cog-1* 3' UTR to repress gene expression.

To support further the notion of *lisy-6*-mediated regulation of *cog-1* expression, we asked whether *lisy-6* alone is sufficient to repress *cog-1* expression in cells that normally express *cog-1* but not *lisy-6*. We ectopically expressed the *lisy-6* hairpin under the control of the *cog-1* promoter (*cog-1^{prom}::lisy-6^{hairpin}*)—which is normally active in several head neurons, uterine cells and vulval cells²¹—and found that ectopic *lisy-6* expression can significantly reduce if not completely abolish *cog-1* expression (Fig. 4f). Expression of a mutated version of *lisy-6* does not show comparable downregulation of *cog-1* expression (Fig. 4f). Taken together, these findings indicate that *lisy-6* is both necessary and sufficient for the regulation of *cog-1* expression.

We ascribe the failure to identify the *lisy-6* miRNA in previously reported genome-wide miRNA searches¹⁴⁻¹⁷ to the following observations. First, although the *C. elegans* and *C. briggsae* *lisy-6* loci are

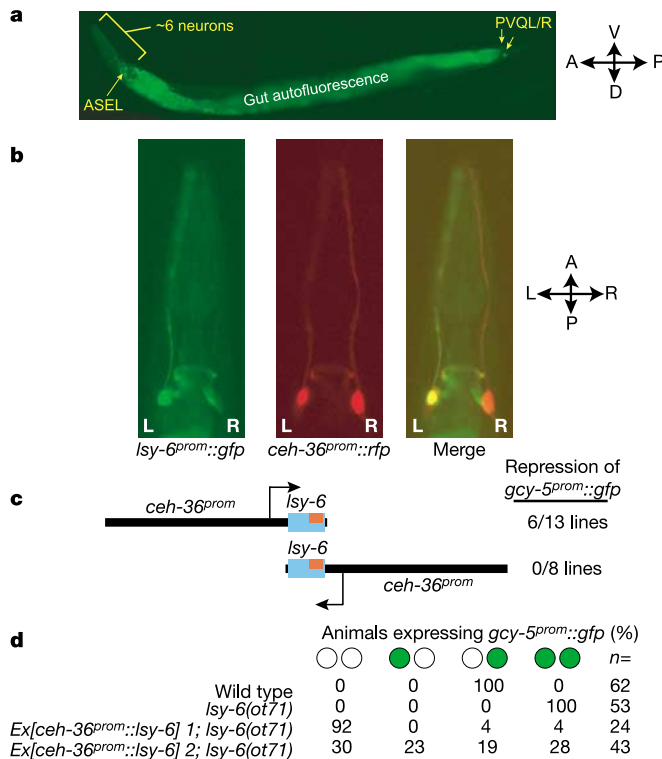


Figure 3 *lisy-6* acts in a highly tissue-specific manner. **a**, Adult transgenic worm expressing *lisy-6^{prom}::gfp*. Neuronal cells expressing *lisy-6^{prom}::gfp* are: ASEL (see **b**), six radially symmetrical head sensory neurons and the PVQL/R tail interneurons. Autofluorescence of gut granules and posterior intestinal background fluorescence are signals in the mid-body region that are not reflective of *lisy-6* expression. Six of six transgenic lines show the same expression pattern. **b**, *lisy-6* is expressed in ASEL but not ASER in adult animals. ASEL and ASER are labelled with a *ceh-36^{prom}::rfp* reporter construct (*otls151*). **c**, The *lisy-6* hairpin driven bilaterally in ASEL/R by the *ceh-36* promoter (*ceh-36^{prom}*) rescues the *lisy-6(ot71)* mutant phenotype in ASEL, as assayed by *gcy-5^{prom}::gfp* expression. **d**, Quantification of the effects of *ceh-36^{prom}::lisy-6^{hairpin}* expression on ASEL and ASER fate in *lisy-6* mutant animals. Two representative lines are shown. A, anterior; D, dorsal; P, posterior; V, ventral.

regulate precise levels of *cog-1* gene expression, thus necessitating an additional level of gene expression control mediated by a miRNA. The elucidation of mechanisms that restrict *lxy-6* expression to just one of two bilaterally symmetrical taste neurons will provide further insights into the molecular mechanisms of establishing left/right asymmetry. □

Methods

Wild-type and mutant strains

We used the following nematode strains: wild-type N2 variation Bristol, CB4856 Hawaiian wild-type isolate, OH2535: *lxy-6*(*ot71*), OH153: *cog-1*(*ot28*), and OH1445: *cog-1*(*ot62*)/+; *otl114*; *him-5*(*e1490*).

Reporter transgenes

We used the following reporter transgenes: *ntl1* *lxy-5^{prom}::gfp*; *lin-15(+)*³, *otl13* *lxy-7^{prom}::gfp*; *lin-15(+)*³, *otl114* *lxy-6^{prom}::gfp*; *rol-6(d)*³, *otl151* *lxy-36^{prom}::rfp*; *rol-6(d)*, and *sy1s63* *lxy-1::gfp*; *dpy-20(+)*²¹. (See Supplementary Information for a description of other transgenic lines.)

DNA construction and injection

All constructs were generated by polymerase chain reaction fusion²². A list of all constructs and primers used can be found in the Supplementary Information. DNA was injected at 2–20 ng μl⁻¹ depending on the experiment (see Supplementary Information) with either *rol-6* (100 ng μl⁻¹) or *unc-122::gfp* (50 ng μl⁻¹) as the injection marker.

Scoring of phenotype

Animals were scored as adults. Quantification of defects shown in the figures can be found in the Supplementary Information.

Received 2 November; accepted 1 December 2003; doi:10.1038/nature02255.
Published online 14 December 2003.

1. Yu, S., Avery, L., Baude, E. & Garbers, D. L. Guanylyl cyclase expression in specific sensory neurons: a new family of chemosensory receptors. *Proc. Natl Acad. Sci. USA* **94**, 3384–3387 (1997).
2. Pierce-Shimomura, J. T., Fautom, S., Gaston, M. R., Pearson, B. J. & Lockery, S. R. The homeobox gene *lim-6* is required for distinct chemosensory representations in *C. elegans*. *Nature* **410**, 694–698 (2001).
3. Chang, S., Johnston, R. J. Jr & Hobert, O. A transcriptional regulatory cascade that controls left/right asymmetry in chemosensory neurons of *C. elegans*. *Genes Dev.* **17**, 2123–2137 (2003).
4. Halpern, M. E., Liang, J. O. & Gamsie, J. T. Leaning to the left: laterality in the zebrafish forebrain. *Trends Neurosci.* **26**, 308–313 (2003).
5. Yost, H. J. Left-right development from embryos to brains. *Dev. Genet.* **23**, 159–163 (1998).
6. Hobert, O., Johnston, R. J. Jr & Chang, S. Left-right asymmetry in the nervous system: the *Caenorhabditis elegans* model. *Nature Rev. Neurosci.* **3**, 629–640 (2002).
7. Bargmann, C. I. & Horvitz, H. R. Chemosensory neurons with overlapping functions direct chemotaxis to multiple chemicals in *C. elegans*. *Neuron* **7**, 729–742 (1991).
8. White, J. G., Southgate, E., Thomson, J. N. & Brenner, S. The structure of the nervous system of the nematode *Caenorhabditis elegans*. *Phil. Trans. R. Soc. Lond. B* **314**, 1–340 (1986).
9. Hobert, O., Tessmar, K. & Ruvkun, G. The *Caenorhabditis elegans* *lim-6* LIM homeobox gene regulates neurite outgrowth and function of particular GABAergic neurons. *Development* **126**, 1547–1562 (1999).
10. Troemel, E. R., Sagasti, A. & Bargmann, C. I. Lateral signaling mediated by axon contact and calcium entry regulates asymmetric odorant receptor expression in *C. elegans*. *Cell* **99**, 387–398 (1999).
11. Wicks, S. R., Yeh, R. T., Gish, W. R., Waterston, R. H. & Plasterk, R. H. Rapid gene mapping in *Caenorhabditis elegans* using a high density polymorphism map. *Nature Genet.* **28**, 160–164 (2001).
12. Lee, R. C., Feinbaum, R. L. & Ambros, V. The *C. elegans* heterochronic gene *lin-4* encodes small RNAs with antisense complementarity to *lin-14*. *Cell* **75**, 843–854 (1993).
13. Olsen, P. H. & Ambros, V. The *lin-4* regulatory RNA controls developmental timing in *Caenorhabditis elegans* by blocking LIN-14 protein synthesis after the initiation of translation. *Dev. Biol.* **216**, 671–680 (1999).
14. Ambros, V., Lee, R. C., Lavanway, A., Williams, P. T. & Jewell, D. MicroRNAs and other tiny endogenous RNAs in *C. elegans*. *Curr. Biol.* **13**, 807–818 (2003).
15. Lim, L. P. et al. The microRNAs of *Caenorhabditis elegans*. *Genes Dev.* **17**, 991–1008 (2003).
16. Grad, Y. et al. Computational and experimental identification of *C. elegans* microRNAs. *Mol. Cell* **11**, 1253–1263 (2003).
17. Lau, N. C., Lim, L. P., Weinstein, E. G. & Bartel, D. P. An abundant class of tiny RNAs with probable regulatory roles in *Caenorhabditis elegans*. *Science* **294**, 858–862 (2001).
18. Johnson, S. M., Lin, S. Y. & Slack, F. J. The time of appearance of the *C. elegans* *let-7* microRNA is transcriptionally controlled utilizing a temporal regulatory element in its promoter. *Dev. Biol.* **259**, 364–379 (2003).
19. Lanjuin, A., VanHoven, M. K., Bargmann, C. I., Thompson, J. K. & Sengupta, P. Otx/otd homeobox genes specify distinct sensory neuron identities in *C. elegans*. *Dev. Cell* **5**, 621–633 (2003).
20. Stark, A., Brennecke, J., Russell, R. B. & Cohen, S. M. Identification of *Drosophila* microRNA targets. *PLoS Biol.* Online publication 13 October 2003 (doi:10.1371/journal.pbio.0000060).
21. Palmer, R. E., Inoue, T., Sherwood, D. R., Jiang, L. I. & Sternberg, P. W. *Caenorhabditis elegans* *cog-1* locus encodes GTX/Nkx6.1 homeodomain proteins and regulates multiple aspects of reproductive system development. *Dev. Biol.* **252**, 202–213 (2002).
22. Hobert, O. PCR fusion-based approach to create reporter gene constructs for expression analysis in transgenic *C. elegans*. *Biotechniques* **32**, 728–730 (2002).

Supplementary Information accompanies the paper on www.nature.com/nature.

Acknowledgements We are grateful to A. Wenick and B. Reinhart for suggestions; Q. Chen for technical assistance; R. Mann, L. Johnston, P. Sengupta and A. Lanjuin for critically reading the manuscript; and the NSF (R.J.J.) and NIH (O.H.) for funding.

Competing interests statement The authors declare that they have no competing financial interests.

Correspondence and requests for materials should be addressed to O.H. (or38@columbia.edu).

.....
A self-organizing system of repressor gradients establishes segmental complexity in *Drosophila*

Dorothy E. Clyde[†], Maria S. G. Corado^{*}, Xuelin Wu[†], Adam Paré, Dmitri Papatsenko & Stephen Small

Biology Department, New York University, New York, New York 10003, USA

^{*} These authors contributed equally to this work

[†] Present addresses: Biosciences Department, University of Kent, Canterbury CT2 7NJ, UK (D.E.C.); Plant Biology Laboratory, The Salk Institute for Biological Studies, La Jolla, California 92037, USA (X.W.)

Gradients of regulatory factors are essential for establishing precise patterns of gene expression during development^{1–3}; however, it is not clear how patterning information in multiple gradients is integrated to generate complex body plans. Here we show that opposing gradients of two *Drosophila* transcriptional repressors, Hunchback (Hb) and Knirps (Kni), position several segments by differentially repressing two distinct regulatory regions (enhancers) of the pair-rule gene *even-skipped* (*eve*). Computational and *in vivo* analyses suggest that enhancer sensitivity to repression is controlled by the number and affinity of repressor-binding sites. Because the *kni* expression domain is positioned between two gradients of Hb, each enhancer directs expression of a pair of symmetrical stripes, one on each side of the *kni* domain. Thus, only two enhancers are required for the precise positioning of eight stripe borders (four stripes), or more than half of the whole *eve* pattern. Our results show that complex developmental expression patterns can be generated by simple repressor gradients. They also support the utility of computational analyses for defining and deciphering regulatory information contained in genomic DNA.

In *Drosophila*, the pair-rule gene *eve* is expressed in a pattern of seven stripes during the syncytial blastoderm stage of development. This pattern foreshadows the mature segmented body plan and is regulated by five enhancers^{4–8}. Three enhancers drive expression of single stripes (*eve* 1, *eve* 2 and *eve* 5), and the remaining two drive expression of pairs of stripes (*eve* 3 + 7 and *eve* 4 + 6). The best characterized *eve* enhancer drives the expression of stripe 2 (*eve* 2)^{9,10}, which is activated in a broad anterior domain by the maternal morphogens Bicoid and Hb. Borders of the stripe are formed by repressive interactions involving the gap proteins Giant (Gt) and Kruppel (Kr), which are expressed in gradients anterior and posterior to the stripe, respectively. Activation and repression are mediated by the direct binding of all four proteins to discrete sites in the enhancer^{9,11}. Thus, this enhancer acts as a transcriptional switch that senses activator/repressor ratios in individual nuclei.

Considerably less is known about the molecular regulation of the enhancers that drive two stripes. *eve* 3 + 7 is activated by ubiquitous factors including dSTAT92E^{12,13}, and activation of *eve* 4 + 6 requires the function of the *fish-hook* gene¹⁴, but other activators are unknown. Genetic studies showed that the gap genes *hb* and *kni* are required for forming the borders of all four of these stripes. *kni* is